

УДК 541.27, 544.163, 544.169

## Quantum Chemical Study of Atomic Structure and Spin States of the $\text{Co}_x(\text{C}_{60})_n$ ( $x=1-8$ , $n=1-3$ ) Complex Nanoclusters

Pavel V. Avramov<sup>a,b\*</sup>, Felix N. Tomilin<sup>a,b</sup>, Alexander A. Kuzubov<sup>a</sup>,  
Polina Artushenko<sup>a</sup> and Sergey V. Kachin<sup>a</sup>

<sup>a</sup> Center of Joint Use of Siberian Federal University,  
79 Svobodny, Krasnoyarsk, 660041 Russia

<sup>b</sup> L.V. Kirensky Institute of Physics SB RAS,  
50 Akademgorodok, Krasnoyarsk, 660036 Russia <sup>1</sup>

Received 20.05.2009, received in revised form 27.05.2009, accepted 04.06.2009

*The main features of the local atomic structure of novel  $\text{Co}_n(\text{C}_{60})_x$  ( $n=1-8$ ,  $x=1-3$ ) complexes and  $\text{Co}_n$  clusters as well were studied using the ab initio GGA calculations for a set of low and high energy isomers in different spin states. It is shown that high-spin low-symmetry structure of free-standing  $\text{Co}_n$  clusters is determined by Jahn-Teller distortions. For the  $\text{Co}(\text{C}_{60})_x$  ( $x=1-3$ ) isomers the spin state  $S=1/2$  is energetically preferable whereas the low energy isomers of  $\text{Co}_2(\text{C}_{60})_x$  ( $x=1-3$ ) have an intermediate spin state of  $S=1$ . The  $\eta^2$  (6-6 edge of  $\text{C}_{60}$ ) type of cobalt ion coordination is preferable for both  $n=1$  and  $n=2$  cases. The  $\eta^2$  (coordination with 6-5 edge) and even the  $\eta^5$  ( $\text{C}_5$  fragment) types serve as low and high energy intermediates for the cobalt ion's migration around the  $\text{C}_{60}$  cage. Formation of cobalt dimers can be the final stage of evolution of  $\text{Co}_n(\text{C}_{60})_x$  atomic structure approaching the equilibrium atomic geometry. For higher  $n$  (3-8) the formation of  $\eta^2$ ,  $\eta^2$  or  $\eta^1$  coordination bonds between  $\text{Co}_n$  fragment and  $\text{C}_{60}$  molecules through carbon hexagons results in stable complex nanoclusters with non-monotonic change of average spin momentum upon the number of cobalt atoms in the  $\text{Co}_n$  cores. The theoretical results are compared with corresponding experimental data.*

*Keywords: Co/ $\text{C}_{60}$  mixtures, local atomic structure, DFT, complex compounds.*

### Introduction

The magnetism of transition metal clusters (TMC) constitutes a fundamental challenge (see, for example, Ref. 1) since atomic and bulk properties are intrinsically different. The TMC physical properties clearly differ from both the atomic and bulk materials [2]: atomic magnetism is due to electrons that occupy localized  $d$ -orbitals, while in the transition metal solids like cobalt, the ferromagnetism properties are caused due to indirect coupling of predominantly

localized  $d$ -like electrons through a small number of itinerant  $d$ -like electrons [3].

The TMCs have been of the significant interest as possible building blocks for magnetic storage and spin-dependent transport devices. For magnetic nanoparticles, this research is stimulated by effort to overcome the supermagnetic limit in magnetic storage devices. Recently, Co- $\text{C}_{60}$  films composed of the Co- $\text{C}_{60}$  compound matrix and Co clusters dispersed therein were found to exhibit an anomalously

\* Corresponding author E-mail address: [paul@iph.krasn.ru](mailto:paul@iph.krasn.ru)

<sup>1</sup> © Siberian Federal University. All rights reserved

large tunnel magnetoresistance (MR) effect as large as 1000% [4-12].

Transition metals, like cobalt, favorably form strong coordination bonds with environments based on carbon. Complex mixtures of  $C_{60}$  fullerenes and transition metals (TM) have attracted attention because of possible applications as promising functional materials (see, for example, [4, 13-14]). The  $TM_x/C_{60}$  composites can be considered condensed complex compounds with incredibly controllable compositions and are the products of various types of vapor co-deposition of transition metals and  $C_{60}$  [4, 15-16]. Actually, the  $TM_x/C_{60}$  composites synthesized using the atomic and molecular beams can be considered as complex mixtures of  $TM_n(C_{60})_m$  compounds. To date, the atomic structure of the  $TM_x/C_{60}$  composites has not been well studied by either experimental or theoretical approaches. The further development of such compounds to obtain novel materials is impossible without detailed theoretical study of the species using sophisticated quantum chemical approaches. In contrary with the  $TM_x/C_{60}$  composites, the  $TM_n(C_{60})_m$  complexes with constant composition are well known objects of coordination chemistry (see, for example, detailed reviews [17-18]) and can be synthesized and characterized using various chemical and spectroscopic methods.

The  $C_{60}$  cages can coordinate metallic ions in different fashions [4, 15]. We denote here the coordination of a metal ion by a 6-6 edge of  $C_{60}$  as an  $\eta^2$  type of coordination. Another possibility is coordination of an ion by a 6-5 edge. We denote this type of coordination as  $\eta^2$  as well. The  $\eta^5$  and  $\eta^6$  types of coordination mean a complex bond between the metal and the  $C_5$  or  $C_6$  fragments of the  $C_{60}$ , respectively. The  $\eta^3$  type means coordination of a metallic ion bonded to a  $C_3$  fragment of the carbon hexagon. And finally the  $\eta^1$  type denotes coordination by one carbon atom of the  $C_{60}$  cage.

For the transition metals, the  $C_{60}$  fullerenes can serve as ligands of different hapticity and exhibit all possible types of coordination ( $\eta^1$ , [17] (Pt-fullerenil radical),  $\eta^2$ , [17-19]  $\eta^3$ , [16, 20]  $\eta^5$ , 21-22 and  $\eta^6$  [18, 23-24]. Some exotic structures like  $C_{60}[\text{Ir}_2\text{Cl}_2(1,5\text{-COD})_2]_2$  may contain up to six metal ions as complex centers [25-28].

In contrast with the cobaltocene  $\text{Co}(\text{C}_5\text{H}_5)_2$ , the  $\text{Co}_x/\text{C}_{60}$  species exhibit either  $\eta^2$  or  $\eta^3$  type of coordination [16, 18-19]. In the work of Ref. 16 the  $\text{Co}_n(\text{C}_{60})_m$  clusters were produced by a combination of laser independent vaporization - of the cobalt and  $C_{60}$  rods - and molecular beam method. The vaporized cobalt and  $C_{60}$  molecules were cooled to room temperature by He carrier gas at 5-7 atm. pressure and then grown into the  $\text{Co}_n(\text{C}_{60})_m$  clusters. For a qualitative study of the atomic structure of the species, mass spectroscopy (MS) method was used in combination with chemical probe analysis. Detailed analysis of the data [16] shows the presence of large or sufficient amounts of the  $C_{60}$ ,  $\text{CoC}_{60}$ ,  $\text{Co}(\text{C}_{60})_2$ ,  $\text{Co}(\text{C}_{60})_3$ ,  $\text{Co}_2(\text{C}_{60})_2$ ,  $\text{Co}_2(\text{C}_{60})_4$ ,  $\text{Co}_3(\text{C}_{60})_4$  and  $\text{Co}_4(\text{C}_{60})_4$  species. The reaction of the species with probe gases ( $\text{CO}$ ,  $\text{O}_2$ ,  $\text{NH}_3$ ) in combination with the mass spectroscopy method allowed authors [16] to make conclusions about the coordination type of the cobalt ions in the  $\text{Co}_n(\text{C}_{60})_m$  complexes.

Although the structural data of work of Ref. 16 is indirect, qualitative and measured for the positively charged clusters (this fact could lead to additional changes in structure and reactivity of the species), it is really important for understanding the structure and properties of the  $\text{Co}_x/\text{C}_{60}$  composites. Combining the mass-spectroscopic data and chemical probe analysis the authors of the work of Ref. 16 show that the cobalt ions in  $\text{Co}_n(\text{C}_{60})_m$  clusters probably exhibit the  $\eta^3$ -type of coordination in some cases, but definitely not  $\eta^5$  or  $\eta^6$  ones. The  $\text{Co}(\text{C}_{60})_2$  cluster is considered [5] to be a bent structure bridged with a Co ion between the fullerene cages, whereas the  $\text{Co}(\text{C}_{60})_3$  cluster

is a triangular planar structure. The  $\text{Co}_4(\text{C}_{60})_4$  has an unusual “composite di-tetrahedral” structure with a  $\text{Co}_4$  pyramid inserted into a  $(\text{C}_{60})_4$  pyramid. Each side of the resulting structure is a  $\text{Co}(\text{C}_{60})_3$  triangle with a cobalt ion between the fullerenes - each vertex of the  $(\text{C}_{60})_4$  tetrahedron belongs simultaneously to 3 different  $\text{Co}(\text{C}_{60})_3$  planes [16]. Actually, the  $\text{Co}_4(\text{C}_{60})_4$  cluster is a tetramer of the  $\text{Co}(\text{C}_{60})_3$  one [16]. In the same sense, the  $\text{Co}_2(\text{C}_{60})_4$  is a dimer and the  $\text{Co}_3(\text{C}_{60})_4$  is a dimer and trimer of the  $\text{Co}(\text{C}_{60})_3$  unit [16]. In the last cases, only two or three  $(\text{C}_{60})_3$  planes of the  $(\text{C}_{60})_4$  tetrahedron contain cobalt ions [16]. Finally, the structure of  $\text{Co}_2(\text{C}_{60})_2$  cluster is considered [16] to be two bridged cobalt ions between two fullerene cages. No evidence of the existence of linear  $\text{Co}-\text{C}_{60}-\text{Co}-\text{C}_{60}$  clusters has been recorded [16].

Several attempts were made to describe – theoretically - the structure and properties of the  $\text{TMC}_{60}$  complexes using empirical tight binding (TB) models and TB based molecular dynamics (MD) simulation technique (see, for examples, Ref. 29-30). Even on the TB level, the structural features of the  $\text{TM}(\text{C}_{60})_2$  and  $\text{TM}_2(\text{C}_{60})_2$  ( $\text{TM}=\text{Ni}, \text{V}$ ) were correctly described in comparison with the existing experimental data [23].

The atomic and electronic structure of the allyl, metallocen, and bis- $\eta^6$  benzene ( $\text{TM}(\text{C}_2\text{H}_4)_n$ ,  $\eta^2$  type of coordination,  $\text{TMCp}_2$ ,  $\eta^5$  type of coordination,  $\text{Cp}=\text{C}_5\text{H}_5$  and  $\text{TMBz}_2$ ,  $\eta^6$  type of coordination,  $\text{Bz}=\text{C}_6\text{H}_6$ , respectively) sandwich complexes with *d*- and *f*-elements and was studied using a more advanced *ab initio* DFT approach [31-38]. It was shown that the DFT theory correctly describes the type of coordination, symmetry and TM-C interatomic distances with high accuracy for all species.

Based on the Becke, Lee, Yang and Parr (BLYP) version of the General Gradient approximation (GGA), a Car-Parrinello MD simulation of the structure and the dynamics of the atomic base of the  $\text{C}_{60}\text{Ta}_3$  system was performed

[38]. It was shown that one Ta ion coordinates with  $\text{C}_{60}$  in a  $\eta^2$  fashion, whereas the  $\text{Ta}_2$  dimer reveals high mobility along the  $\text{C}_{60}$  cage. The ease of migration of the  $\text{Ta}_2$  fragment around the  $\text{C}_{60}$  cage is the main structural peculiarity of the  $\text{C}_{60}\text{Ta}_3$  complex.

The conditions of synthesis [15] for  $\text{Co}_x/\text{C}_{60}$  composites, using atomic and molecular beams with consequent condensation of the mixtures imply, that all possible types (both low and high energy species) of local atomic structures could be formed during the experiment. Because of this, the atomic structure of the species can evolve during - or shortly after - the synthesis to achieve relatively stable positions of the cobalt ions and the  $\text{C}_{60}$  cages. Migration of the Co ions around and between the fullerene cages is the most probable mechanism to achieve this. The first step to study the atomic structure evolution process is to find all possible local  $\text{Co}_n(\text{C}_{60})_m$  isomers and intermediates. From a general point of view, hundreds of  $\text{Co}_n(\text{C}_{60})_m$  structures in low and high energy and spin states can be realized. Unfortunately, due to the big number and complexity of the structures (hundreds of atoms including several TMs) it is hardly possible to find appropriate transition states on the isomerization reaction pathways. Because of this, we can only judge the atomic structure evolution of the  $\text{Co}_x/\text{C}_{60}$  composites based on the information about the atomic structure of all possible isomers and intermediates.

Presented here is a systematic theoretical *ab initio* DFT investigation of the atomic structure evolution of the  $\text{Co}/\text{C}_{60}$  composites in terms of the structure and energetic characteristics of a number of  $\text{Co}_n(\text{C}_{60})_m$  clusters. This study is organized as follows: Section II describes the computational methods and objects under investigation, followed by results and discussion in Section III. Conclusions are presented in Section IV.

### Computational details

The *Gaussian 03* [39] code was used to calculate the electronic structure of  $\text{Co}_n(\text{C}_{60})_m$  clusters as well as free standing  $\text{Co}_n$  clusters. Geometry optimization was performed by using the analytic energy gradients at a B3LYP/6-31G\* level of theory [40] and GGA PBE approximation. [41, 42] as well. It has been shown that the PBE potential gives good results for metallic systems, [43] which is important for the  $\text{Co}_x$  clusters.

All relative energies were calculated taking into account the basis set superposition error (BSSE). Based on the electronic structure calculations of the  $\text{Co}_n(\text{C}_{60})_m$  clusters at the GGA/6-31G\* level for the  $\text{Co}_n(\text{C}_{60})_m$  systems the BSSE was estimated in the range 35 – 55 kcal/mol. Taking the BSSE corrections into account is really important to predict the correct energy values and relative stability of the species.

To study the atomic and electronic structure of the metallocene systems, [31] HF approach as well as a wide variety of DFT potentials (BHLYP, B3LYP, BLYP, BP86, LSDA) were used. It was shown [31] that the B3LYP method [40] gives the best results among the approximations listed above. At present, the B3LYP method is probably the best tested approach among all *ab initio* DFT ones. It was designed [40] especially for correct description of the dissociation limit of a wide variety of molecules. The accuracy of the B3LYP method in describing the dissociation energies estimated for the G2 set is equal to 3.5 kcal/mol [40, 44-45].

The free-standing  $\text{Co}_x$  clusters were allowed to change freely during atomic structure optimization without symmetry restrictions. Some initial structural types for geometry optimization were taken from Refs. 48-51. All possible spin states were tested to discover the

ground states of the  $\text{Co}_x$  clusters at GGA PBE/6-31G\* level of theory.

The atomic structure of  $\text{Co}_x/\text{C}_{60}$  systems is characterized by its complexity [4, 15-16]. Only general information such as Co-C interatomic distances and possible coordination numbers, can be extracted from the structural spectroscopic experiments [15-16]. The unique atomic structure of  $\text{C}_{60}$  cage and the synthesis conditions are the reasons for the complex and irregular nature of the  $\text{Co}_x/\text{C}_{60}$  composites [15]. At the local atomic structure level, this should reveal [16] a large variety of possible coordination types of cobalt ions with close or equal coordination numbers. A large variety of interatomic distances and different spin states should also be found. The presence of the transition metal ions and partially negative charges of the fullerene cages (because of the oxidation of the cobalt ions by  $\text{C}_{60}$  [52]) should be followed by the electronic correlations [53]. As the result of all factors described above, no symmetry restrictions can be applied *a priori* to the  $\text{Co}_n(\text{C}_{60})_m$  clusters. The complexity of the objects and a great number of possible isomers in different spin states make it hardly possible - without taking into account of available experimental data and some basic features of atomic structure of  $\text{C}_{60}$  cages – a theoretical design of the preliminary structural models of the  $\text{Co}_n(\text{C}_{60})_m$  clusters.

To study the atomic structure of the  $\text{Co}/\text{C}_{60}$  species, we theoretically designed a number of  $\text{Co}_n(\text{C}_{60})_m$  clusters with  $n=1-8$  and  $m=1-3$  with all possible coordinations of the cobalt ions and  $\text{C}_{60}$  sites. Such restrictions of the  $n$  and  $m$  numbers are based on the previous experimental study of the species presented in the work of Ref. 16. For the  $\text{Co}1$  systems ( $\text{Co}(\text{C}_{60})_2$  and  $\text{Co}(\text{C}_{60})_3$  clusters) all possible types of coordination ( $\eta^6$ ,  $\eta^5$ ,  $\eta^3$ ,  $\eta^2$ ,  $\eta^2$  and  $\eta^1$ ) in low ( $S=1/2$ ) and middle ( $S=3/2$ ) spin states were chosen as initial types of structures. Later, we will show that - for the neutral  $\text{Co}1$

systems - the low  $S=1/2$  state is energetically preferable.

To study the atomic structure of the  $\text{Co}/\text{C}_{60}$  systems with higher indexes ( $x=3-8$  and  $n=1-3$ ) we designed a number of  $\text{Co}_x(\text{C}_{60})_n$  clusters with all possible spin states and  $\eta^2$ ,  $\eta^{2'}$  and  $\eta^1$  coordination types for the cobalt ions. In general, the  $\text{Co}_x$  cores can be coordinated with  $\text{C}_{60}$  cages through 1, 2, 3 or even 4 cobalt ions, so, the notations for the complex interfaces between the  $\text{Co}_x$  and  $\text{C}_{60}$  parts can be designed using up to four  $\eta^k$  characters.

To compare the theoretical results with the experimental mass-spectroscopic and chemical probe method data, [16] we performed calculations on positively charged  $\text{Co}^+$  clusters in low ( $S=0$ ) and middle ( $S=1$ ) spin states. It was shown that the low ( $S=0$ ) spin state is preferable for such types of objects. Finally, the structure of 89  $\text{Co}_n(\text{C}_{60})_m$  ( $n=1, 2, m=2, 3$ ) neutral and positively charged clusters in low and intermediate spin states were determined at the B3LYP/6-31G\* level.

No high energy  $\eta^6$  isomers or intermediates have been determined in our B3LYP/6-31G\* calculations. We have determined the atomic structure of only a couple of isomers of the  $\eta^3$ -type of coordination.

Each  $\text{C}_{60}$  site has its own coordination type with a cobalt ion. For the  $n=1$ , we introduced special notations for the mixed structures like  $\eta^2/\eta^2$  (coordination of a cobalt ion by two 6-6 edges of different  $\text{C}_{60}$  cages),  $\eta^2/\eta^{2'}$  (one 6-6 and one 6-5 edge),  $\eta^2/\eta^5$  (the 6-6 edge and  $\text{C}_5$  fragment) and  $\eta^5/\eta^5$  (two  $\text{C}_5$  fragments). For the  $n=1$  no  $\eta^5/\eta^{2'}$ ,  $\eta^2/\eta^3$ ,  $\eta^2/\eta^{2'}$ ,  $\eta^3/\eta^{2'}$ ,  $\eta^3/\eta^3$  or  $\eta^3/\eta^5$  structures were detected.

The case of  $n=2$  is more complex: it is necessary to consider the coordination types of both cobalt ions. For the  $n=2$ , the  $\eta^5$  fashion can be realized only in the case of one bridged cobalt ion between the  $\text{C}_{60}$  cages. Later we will show that such type of structure have really high relative energies. For the  $m$  and  $n=2$  all possible

combinations of  $\eta^2$  and  $\eta^{2'}$  types of coordination ( $\eta^2:\eta^2/\eta^2:\eta^2$ ,  $\eta^2:\eta^{2'}/\eta^2:\eta^2$ ,  $\eta^{2'}:\eta^{2'}/\eta^2:\eta^2$ ,  $\eta^{2'}:\eta^2/\eta^2:\eta^2$ ,  $\eta^2:\eta^2/\eta^2:\eta^{2'}$  and  $\eta^{2'}:\eta^2/\eta^2:\eta^{2'}$ , the colon separates coordination types of both cobalt ions within the same  $\text{C}_{60}$  cage whereas the slash symbol separates different  $\text{C}_{60}$  sites) were determined as well as two high energy mixed isomers with  $\eta^3:\eta^2/\eta^2:\eta^2$  and  $\eta^3:\eta^2/\eta^3:\eta^2$  types (the last structure has two additional  $sp^3$  C-C bond between the  $\text{C}_{60}$  cages). By keeping the initial nature of the cobalt ion's coordination fashion, the number of possible isomers of  $\text{Co}_2(\text{C}_{60})_2$  in different spin states becomes really large (several dozens) because the relative positions of the  $\text{C}_{60}$  cages can be different.

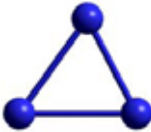
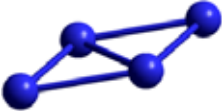
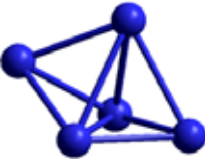

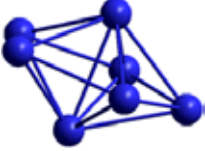

The linear or bent  $\text{Co}_2(\text{C}_{60})_3$  structures mostly manifest the  $n=1$  types of coordination because of the absence of direct Co-Co interactions like in  $\text{Co}_2(\text{C}_{60})_2$  systems. In general, there are only a few unequivalent Co - Co positions which differ from each other by the Co - Co distance and coordination fashion. Like in the case of  $n=1$ , the  $\eta^2$  type of coordination ( $\eta^2/\eta^2:\eta^2/\eta^2$ , the  $\eta^2/\eta^2$  type of coordination for both cobalt ions) has the lowest energy. The  $\eta^2/\eta^2:\eta^2/\eta^{2'}$  fashion is the second in energy and the  $\eta^5/\eta^5:\eta^5/\eta^5$  one has the highest energy. Energetically, the mixed structures (such as  $\eta^5/\eta^5:\eta^5/\eta^2$  or  $\eta^2/\eta^5:\eta^5/\eta^2$  etc.) are between them.

## Results and discussion

### a) $\text{Co}_x$ free-standing cores

The information of the atomic structure and spin state of free  $\text{Co}_x$  clusters is summarized in Table 1. The PBE/6-31G\* results qualitatively correspond to the previously published DFT (mostly different types of GGA approximation) [49-50] and TB [48, 51] data for free-standing cobalt clusters giving the same symmetries but sometimes different orders of the  $\text{Co}_x$  isomers. Unfortunately the authors of [48, 51] did not publish the key interatomic distances and angles,

Table 1. Symmetry, interatomic distances (Å) and the number of unpaired spins of the ground states of the  $\text{Co}_x$  clusters

Composition	General view	Symmetry	Interatomic distances, Å	Number of unpaired spins (spin/atom)
$\text{Co}_3$		$C_{2v}$	2.189 1.998	9 (3)
$\text{Co}_4$		$C_{2h}$	2.288 2.119	10 (2.5)
$\text{Co}_5$		$C_s$	2.248 2.153 2.129 2.103	13 (2.6)
$\text{Co}_6$		$C_i$	2.215 2.214 2.213	14 (2.33)
$\text{Co}_7$		$C_s$	2.275-2.186	15 (2.14)
$\text{Co}_8$		$C_s$	2.306-2.182	16 (2)

so we can not make direct comparison of the atomic structures in this work. For example, the TB results [48, 51] give the same symmetries of global minima for  $\text{Co}_6$ , and  $\text{Co}_7$  clusters, whereas for the rest of them the TB treats the second in energy isomers at PBE level of theory as ground states. The BLYP [49-50] gives the same symmetries of ground states for  $\text{Co}_4$ ,  $\text{Co}_5$  and  $\text{Co}_6$  clusters predicting different energy order for  $\text{Co}_3$ ,  $\text{Co}_7$  and  $\text{Co}_8$  clusters. Atomic coordinates of all free-standing cobalt cores can be downloaded

from Supporting Information section of the JPCC website.

The Jahn-Teller effect plays an important role in the symmetry lowering of the free-standing  $\text{Co}_x$  cores due to correlation effects in rich  $\text{Co}-d$  shells of the clusters. The species display only low-symmetry groups ( $C_{2v}$  ( $\text{Co}_3$ ) and  $C_s$  ( $\text{Co}_4$ ,  $\text{Co}_5$  and  $\text{Co}_8$ )) or total absence of symmetry ( $\text{Co}_6$  and  $\text{Co}_7$  clusters) with significant variations of interatomic Co-Co distances (Table 1). It is necessary to note that a  $\text{Co}_3$  cluster configuration with 7 unpaired

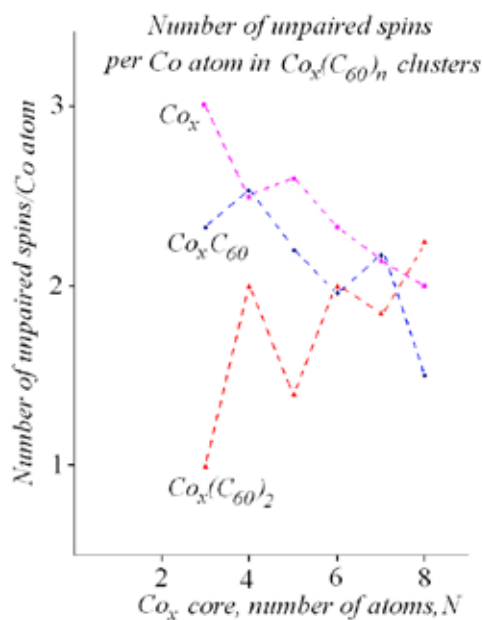


Fig. 1. Number of unpaired spins per cobalt atom in  $\text{Co}_x$  cores of  $\text{Co}_x(\text{C}_{60})_n$  nanoclusters. Pink squares denote the free-standing  $\text{Co}_3$ ,  $\text{Co}_4$ ,  $\text{Co}_5$ ,  $\text{Co}_6$ ,  $\text{Co}_7$  and  $\text{Co}_8$  clusters. Blue diamonds denote  $\text{Co}_3\text{C}_{60}$ ,  $\text{Co}_4\text{C}_{60}$ ,  $\text{Co}_5\text{C}_{60}$ ,  $\text{Co}_6\text{C}_{60}$ ,  $\text{Co}_7\text{C}_{60}$  and  $\text{Co}_8\text{C}_{60}$ . Red triangles denote  $\text{Co}_3(\text{C}_{60})_2$ ,  $\text{Co}_4(\text{C}_{60})_2$ ,  $\text{Co}_5(\text{C}_{60})_2$ ,  $\text{Co}_6(\text{C}_{60})_2$ ,  $\text{Co}_7(\text{C}_{60})_2$  and  $\text{Co}_8(\text{C}_{60})_2$ . Three dashed lines are the guides to eyes

spins is only 0.6 kcal/mol higher in energy than the lowest energy isomer with multiplicity equal to 10 (9 unpaired spins).

The increase in size (or, what is the same, the number of cobalt atoms) of the species leads to a visible decrease in number of unpaired spins per cobalt atom. A non-monotonic dependence of the average number of unpaired spins per cobalt atom (Fig. 1) displays a local maximum for  $\text{Co}_5$  cluster, which is close to the results of the previous works [48-51]. For example, the GGA approach [49-50] gives the same dependence with one maximum for  $\text{Co}_6$  cluster (instead  $\text{Co}_5$  in our case). The TB results [48, 51] also display maximum for  $\text{Co}_6$ .

#### a) $\text{Co}(\text{C}_{60})_2$ and $\text{Co}(\text{C}_{60})_3$ clusters

Tables 2 and 3 present the relative energies, types of coordinations and structural images (general and closest cobalt neighborhood) of all

$\text{Co}(\text{C}_{60})_2$  and  $\text{Co}(\text{C}_{60})_3$  (Table 2) as well as  $\text{Co}(\text{C}_{60})_2^+$  and  $\text{Co}(\text{C}_{60})_3^+$  (Table 3) clusters in low spin states ( $S=1/2$  and 0 respectively). On the B3LYP/6-31G\* level the doublet – quartet splitting for the neutral systems is from 2.5 kcal/mol ( $\eta^5/\eta^5$  complex) to 36.4 ( $\eta^2/\eta^2$  complex) kcal/mol. Because of this, we present the data of the low spin states only. All relative energies were calculated taking into account the basis set superposition error. The left/lower carbon atoms are in black, the right/upper carbon fragments are shown in green/blue and the cobalt atom is in red.

Even though the positively charged clusters cannot play any role in the formation of the local atomic structures of  $\text{Co}_x/\text{C}_{60}$  composites, they can be used as test systems to check the accuracy of the quantum chemical calculations. The theoretical B3LYP/6-31G\* atomic structure of positively charged systems confirms the indirect experimental results [16] shown in Table 3: the  $\text{Co}(\text{C}_{60})_2^+$  has a bent structure and the formation of additional Co-C bonds ( $\text{Co}(\text{C}_{60})_3^+$  complex, with absolute minimum or zero relative energy) which sufficiently lowers the energy of the cluster (19.0 kcal/mol). Creation of an additional C-C  $sp^3$  bond between the  $\text{C}_{60}$  cages ( $\text{Co}(\text{C}_{60})_2^+$  with C-C bond) lowers the relative energy up to 7.6 kcal/mol above 0 and makes the bent angle bigger. Creation of additional C-C  $sp^3$  bonds between the  $\text{C}_{60}$  cages ( $\text{Co}(\text{C}_{60})_3^+$  with additional 6 C-C bonds) does not change the energy of the system (0.3 kcal/mol on 6-31G\* level). The lowest in energy -  $\text{Co}(\text{C}_{60})_3^+$  cluster - has triangular planar structure like in the work of Ref. 16 with  $\eta^2/\eta^2/\eta^2$  type of coordination (which is common for the cobalt-fullerene complexes) [18]. We have determined some additional types of coordination such as  $\eta^2/\eta^2$  (see above the Computation Details Section) as well as  $\eta^5/\eta^5$  and  $\eta^2/\eta^5$  ones. These isomers have high relative energies (up to 41 – 29 kcal/mol for the neutral systems). In spite of the  $\eta^5/\eta^5$  isomer having the highest energy, this type of

Table 2. Coordination Types, structures and relative energies (kcal/mol) of  $\text{Co}(\text{C}_{60})_2$  and  $\text{Co}(\text{C}_{60})_3$  clusters ( $S=1/2$ ). All relative energies were calculated taking into account basis set superposition error. The left/lower carbon atoms are in black, the right/upper carbon fragments are shown in green/blue and cobalt is in red

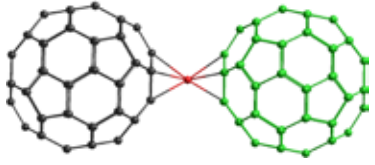
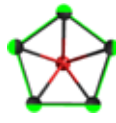
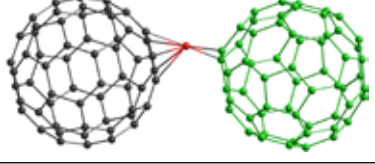
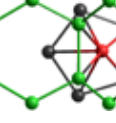
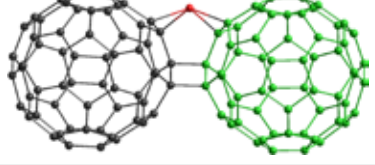
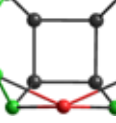
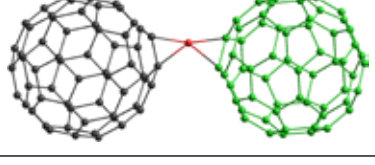
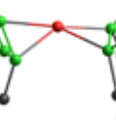
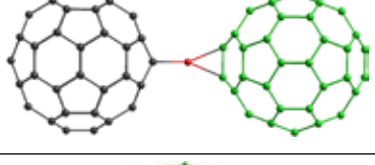
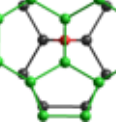
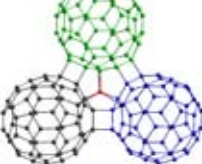
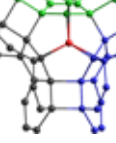
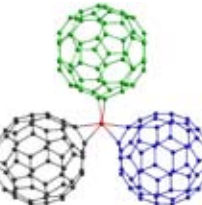
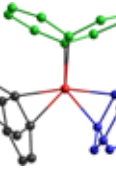
Type of coordination	General view	Closest cobalt neighborhood	Relative Energy (kcal/mol)
$\eta^5/\eta^5$			41.4
$\eta^2/\eta^5$			32.8
$\eta^2/\eta^2$ with one C-C bond			30.5
$\eta^2/\eta^2$			28.9
$\eta^2/\eta^2$			15.2
$\eta^2/\eta^2/\eta^2$ with 3 C-C bonds			13.3
$\eta^2/\eta^2/\eta^2$			0.0



Table 3. Types of coordinations, structures and relative energies (kcal/mol) of  $\text{Co}(\text{C}_{60})_2^+$  and  $\text{Co}(\text{C}_{60})_3^+$  clusters (S=0). All relative energies were calculated taking into account basis set superposition error. The left/lower carbon atoms are in black, the right/upper carbon fragments are shown in green/blue and cobalt is in red

Type of coordination	General view	Closest cobalt neighborhood	Relative Energy (kcal/mol)
$\eta^2/\eta^2$			19.0
$\eta^2/\eta^2$			17.4
$\eta^5/\eta^5$			8.9
$\eta^2/\eta^2$ with one C-C bond			7.6
$\eta^2/\eta^5$			5.2
$\eta^2/\eta^2/\eta^2$ with 3 C-C bonds			0.3
$\eta^2/\eta^2/\eta^2$			0.0

coordination was detected in the works of Refs. 21 and 22 and explained [36-37] by stabilization of the  $\eta^5$  position by some saturation groups on the outer surface of fullerenes.

A comparison of the positively charged systems (Table 3) and the neutral systems (Table 2) shows that ionization can cause some energetic and structural changes. For example, the staggered  $\eta^2/\eta^2$  and  $\eta^2/\eta^2/\eta^2$  (three 6-6 edges) types of coordination are preferable for the neutral  $\text{Co}(\text{C}_{60})_n$  ( $n=2, 3$ ) clusters. Formation of additional C-C bonds between the fullerenes sufficiently increases the energy of the clusters (as low as 13.3 kcal/mol for  $\text{Co}(\text{C}_{60})_3$  and as high as 30.5 kcal/mol for and  $\text{Co}(\text{C}_{60})_2$  clusters). The eclipsed  $\eta^2/\eta^2$  configuration of the  $\text{Co}(\text{C}_{60})_2^+$  cluster has the highest energy (Table 3). Ionization results not only in the changing of relative stability of the system, but in the symmetry state as well.

Comparison of the atomic structure of the zero energy  $\text{Co}(\text{C}_{60})_3$  cluster with the structural XAFS data [15] shows that B3LYP/6-31G\* calculations (Table 2) can correctly describe both the coordination number for the  $\text{Co}_x/\text{C}_{60}$  composites (equal to 6 for the  $\text{Co}(\text{C}_{60})_3$  cluster) and the Co-C interatomic distance with good accuracy (2.01 Å is the experimental value and 2.06 Å the theoretical one). Formation of the additional Co-C complex bonds (transition from a  $\text{Co}(\text{C}_{60})_2$  system to a  $\text{Co}(\text{C}_{60})_3$  system) decreases the energy up to 15.2 kcal/mol. The  $\text{Co}(\text{C}_{60})_2$  clusters with different types of coordination ( $\eta^2/\eta^2$ ,  $\eta^2/\eta^5$  and  $\eta^5/\eta^5$ ) have sufficiently higher relative energies (from 28.9 up to 41.4 kcal/mol).

#### b) $\text{Co}_2(\text{C}_{60})_2$ clusters

Only three structural types of  $\text{Co}_2(\text{C}_{60})_2$  clusters can be realized due to the specific atomic structure of  $\text{C}_{60}$  cage. The first one can be characterized by existence of cobalt dimers bonding the  $\text{C}_{60}$  cages. The  $\text{C}_{60}$  cages of the second type can be bounded by both cobalt ions

without formation of a metallic dimer, due to the possible formation of additional C-C bonds between fullerene cages. The  $\text{C}_{60}$  cages of the third type can be bonded by one cobalt ion only, whereas the second ion coordinates with only one  $\text{C}_{60}$  cage. Later we will show that the second and the third types of clusters have high relative energies (~50 - 100 kcal/mol).

The B3LYP/6-31G\* calculations show that low energy  $\text{Co}_2(\text{C}_{60})_2$  isomers have the triplet spin state (Table 4). We determined 27  $\text{Co}_2(\text{C}_{60})_2$  isomers in the triplet state and 28  $\text{Co}_2(\text{C}_{60})_2$  ones in the singlet state within all three types. All isomers in the triplet state keep the main peculiarities of the atomic structure of the singlet analogs such as type of coordination, relative positions of  $\text{C}_{60}$  cages and Co-C distance (~1.9 ÷ 2.1 Å). The typical singlet-triplet splitting for all isomers is equal to 40 - 70 kcal/mol. The transition from singlet to triplet state leads only in enlarging the Co-Co distance of cobalt dimers by approximately 0.2 ÷ 0.5 Å.

Some of the  $\text{Co}_2(\text{C}_{60})_2$  isomers are presented in Table 4. The cobalt ions in metallic dimers present the  $\eta^2$  and  $\eta^2$  or, in less extent cases, the  $\eta^3$  types of coordination (see Table 4). The atomic structure of the 3 lowest energy isomers (isomers 1, 2 and 3, S=1) clearly confirm the indirect structural data [5] - two cobalt ions between the  $\text{C}_{60}$  cages. Formation of the cobalt dimers is energetically preferable, even in the case of formation of additional C-C  $sp^3$  bonds between the  $\text{C}_{60}$  cages (isomers 5 and 6). This fact is really important to understand the structures and properties of the  $\text{Co}_x/\text{C}_{60}$  composites. In some extent, during synthesis [4] such  $\text{Co}_2(\text{C}_{60})_2$  complexes can be realized because of radical character of  $\text{C}_{60}$  cages with attached metal ions. [34] Once formed, they can prevent the system from changing the positions of the cobalt ions because of the high energy required to destroy the additional  $sp^3$  C-C bonds between the  $\text{C}_{60}$  cages.

Table 4. Types of coordinations, structures and relative energies (kcal/mol) of some  $\text{Co}_2(\text{C}_{60})_2$ . All relative energies were calculated taking into account basis set superposition error. The lower carbon atoms are in black, the right/upper carbon fragments are shown in green and cobalt is in red

Number	General view	Detailed view	Coordination type	Energy (kcal/mol)	$R_{\text{Co-Co}}$ , Å
1	2	3	4	5	6
1 (S=1)			$\eta^2:\eta^2/\eta^2:\eta^2$	0	2.73
2 (S=1)			$\eta^2:\eta^2/\eta^2:\eta^2$	9.4	2.98
3 (S=1)			$\eta^2:\eta^2/\eta^2:\eta^2$	19.1	2.973
4 (S=1)			$\eta^3:\eta^2/\eta^2:\eta^2$ (65:66:65/66:66)	30.4	2.41
5 (S=1)			$\eta^2:\eta^2/\eta^2:\eta^2$	49.0	3.21
6 (S=1)			$\eta^3:\eta^2/\eta^3:\eta^2$ (66:66:65/66:66:65)	80.3	5.61

The three lowest energy isomers are characterized by  $\eta^2$  and  $\eta^2$  coordination type. The  $C_{60}$  cages of the first isomer (relative energy 0 kcal/mol) are connected by a cobalt dimer through two  $C_6$  fragments of both fullerenes (Table 4). The first  $C_{60}$  cage bonds with the  $Co_2$  fragment through the middle of the  $C_6$  fragments using 6-6 and 6-5 edges, whereas the second fullerene bonds with the  $Co_2$  through two 6-6 edges ( $\eta^2:\eta^2/\eta^2:\eta^2$  coordination type). The second isomer has the relative energy equal to 9 kcal/mol and has an  $\eta^2:\eta^2/\eta^2:\eta^2$  type of coordination of the  $Co_2$  fragment through four 6-6 edges of the  $C_6$  fragment. The third isomer has the relative energy equal to 19.1 kcal/mol and an  $\eta^2:\eta^2/\eta^2:\eta^2$  type of coordination through two  $C_6$  fragments. In this case the  $Co_2$  dimer connects with two 6-6 edges of one  $C_6$  fragment and with two 6-5 edges of the second one. All other  $\eta^2$ -type isomers have higher relative energies (from 23 up to 120 kcal/mol) and can be obtained by combining all possible coordinations of the two  $C_{60}$  cages and  $Co_2$  fragment.

Two isomers of  $Co_2(C_{60})_2$  clusters (numbers 4 and 6, Table 4) reveal the  $\eta^3$ -type of coordination through a specific point on the  $C_6$  fragment surface. Both isomers can only play some role during the atomic structure evolution because of the high relative energies (30 and 80 kcal/mol correspondingly).

The initial presence of a wide set of  $Co_2(C_{60})_2$  clusters in the  $Co_x/C_{60}$  mixtures<sup>4</sup> with similar energies can be followed by the process of isomerization (the Co ions hopping through the  $\eta^2$ ,  $\eta^2$  and  $\eta^3$ -points on the surface of the  $C_{60}$  cages). The  $\eta^2:\eta^2/\eta^2:\eta^2$  and  $\eta^2:\eta^2/\eta^2:\eta^2$  types of coordination are preferable, but other high energy isomers can play some role as intermediate complexes in the process. Formation of additional C-C bonds between the  $C_{60}$  cages is not energetically preferable but may occur. If this happens, the new bonds should prevent the

migration of the cobalt ions around the fullerene cages.

### c) $Co_2(C_{60})_3$ clusters

As it was mentioned in the Introduction and Computational Details sections, the linear or bent  $Co_n(C_{60})_m$  clusters were not detected in the MS experiment [16]. Because of presence of other types of high clusters like  $Co_2(C_{60})_2$ ,  $Co_2(C_{60})_4$ ,  $Co_3(C_{60})_4$  and  $Co_4(C_{60})_4$ , one would imagine the probability of the random formation of the linear/bent  $Co_2(C_{60})_3$  structures should be sufficiently higher than zero. The absence of the  $Co_2(C_{60})_3$  clusters and high amount of the  $Co_2(C_{60})_2$  ones can be partly explained by the fast transformation of  $Co_2(C_{60})_3$  to  $Co_2(C_{60})_2$ . This occurs when the cobalt ions migrate around the central  $C_{60}$  cage, followed by the removal of one  $C_{60}$  when a double bridged  $Co_2(C_{60})_2$  cluster is formed.

To study the atomic structure evolution of  $Co_x/C_{60}$  composites, we calculated four sets of  $Co_2(C_{60})_3$  clusters to model the process of cobalt ion migration around the  $C_{60}$  cages. Based on the calculations for the Co1 systems (Table 2), we propose the  $\eta^2/\eta^2:\eta^2/\eta^2$  and  $\eta^2/\eta^2:\eta^2/\eta^2$  types of coordination of  $Co_2(C_{60})_3$  clusters as energetically preferable and the pure  $\eta^5/\eta^5:\eta^5/\eta^5$  and mixed  $\eta^5/\eta^5:\eta^5/\eta^2\eta^5$  as the ones highest in energy. It is necessary to note that regardless of the high energy of the species, during the chemical synthesis, [4] even the  $\eta^5/\eta^5:\eta^5/\eta^5$  and  $\eta^5/\eta^5:\eta^2/\eta^5$  intermediates can play some role in the  $Co_x/C_{60}$  composite characterization.

The conformable  $\eta^5/\eta^5:\eta^5/\eta^5$  and  $\eta^5/\eta^5:\eta^5/\eta^2\eta^5$  complexes, with close Co-Co distances, are 10-15 kcal/mol higher in energy than the  $\eta^2/\eta^2:\eta^2/\eta^2$  and  $\eta^2/\eta^2:\eta^2/\eta^2$  ones (Tables 5 and 6). The smaller the Co-Co distance the lower the energy of the  $\eta^5$ -type complexes. However, the  $\eta^5$  structures are not suitable for the formation of the cobalt dimer structures because of features of the atomic structure of the species. The formation of the

Table 5. Structures and relative energies (kcal/mol) of  $\eta^2:\eta^2:\eta^2$ -type  $\text{Co}_2(\text{C}_{60})_3$  clusters. All relative energies were calculated taking into account basis set superposition error

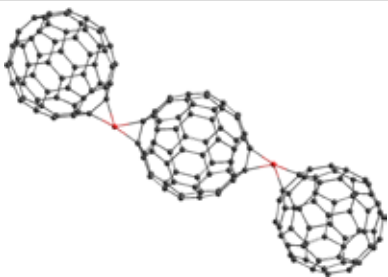
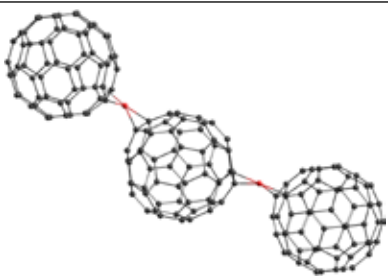
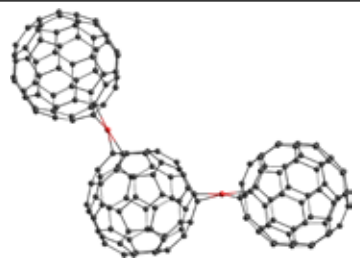
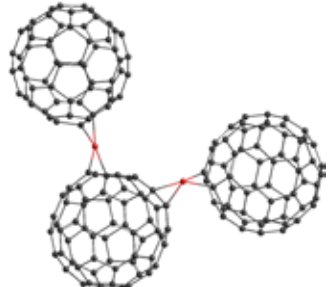
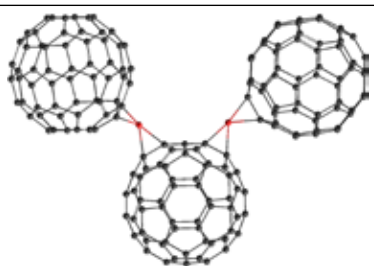
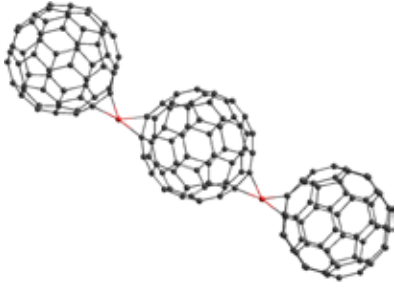
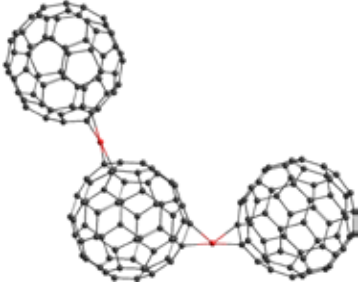
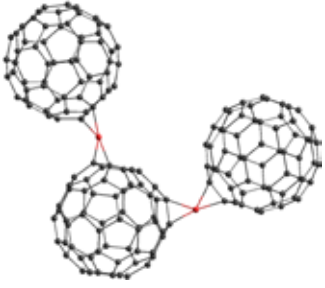
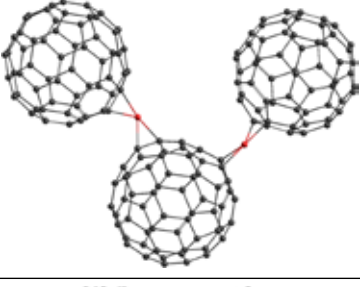
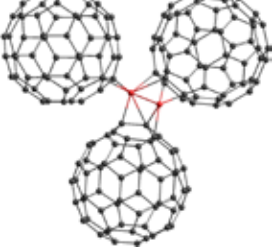
Number	General View	Relative Energy (kcal/mol)	$R_{\text{Co-Co}}$ , Å
1		35.3	10.728
2		34.3	10.179
3		36.2	8.579
4		38.0	6.054
5		34.4	5.231

Table 6. Structures and relative energies (kcal/mol) of  $\eta^2:\eta^2/\eta^2:\eta^2$ -type  $\text{Co}_2(\text{C}_{60})_3$  clusters. All relative energies were calculated taking into account basis set superposition error

Number	General View	Relative Energy (kcal/mol)	$R_{\text{Co-Co}}$ , Å
1		43.0	10.495
2		48.6	9.529
3		49.2	7.593
4		43.5	6.420
5		42.4	2.530

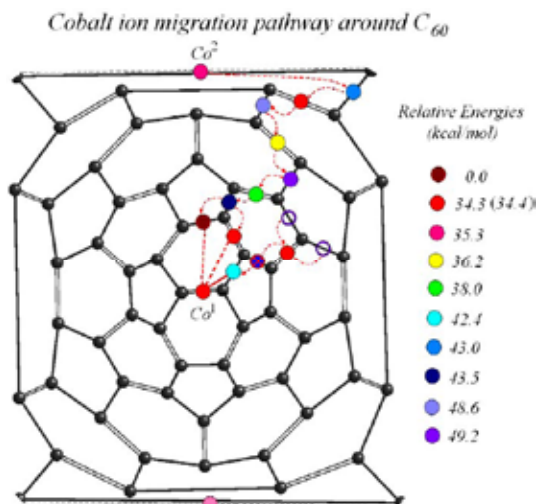


Fig. 2. Schlegel diagram of cobalt ions migrating around the central  $C_{60}$  cage of the  $Co_2(C_{60})_3$  type of clusters. The first cobalt ion (red dot  $Co^1$ ) has a fixed position and is placed in the center of the 6-6 edge. The initial position of the second cobalt ion (pink dot  $Co^2$ ) is in the center of the opposite 6-6 edge. Migration of the second cobalt ion around  $C_{60}$  cage, through 6-5 and 6-6 edges, is presented by red broken arrows and color dots reflecting the relative energies of isomers ( $\eta^2:\eta^2/\eta^2:\eta^2$  type of coordination) and intermediates ( $\eta^2:\eta^2/\eta^2:\eta^2$  type of coordination). The carbon atoms are presented in black. The two lowest and highest carbon atoms are equivalent and presented as half circles because of the specific Schlegel diagram projection. The  $Co^2$  has a mirror image in the bottom of the figure (light pink dot) as well as the 6-6 edge bonded with it. Two violet empty circles denote the beginning of an alternative reaction pathway of the cobalt migration. The traffic sign “do not stop” denote absence of the intermediate state on the particular 6-5 edge

dimer structures, such as isomer 1 of  $Co_2(C_{60})_2$  (Table 4), requires sufficient rearrangement of the cobalt ion's coordination type - from  $\eta^5$  to  $\eta^2$  ones and from  $\eta^5$  to  $\eta^{2'}$  ones. Because of this the  $\eta^5$  complexes cannot play any role as direct precursors in the formation of cobalt dimers.

The  $\eta^2:\eta^2:\eta^2/\eta^2$  and mixed  $\eta^2:\eta^2:\eta^2/\eta^{2'}$  types of  $Co_2(C_{60})_3$  structures have the lowest energy among the  $Co_2(C_{60})_3$  clusters. The energy dependence of the  $\eta^2:\eta^2:\eta^2/\eta^2$  clusters upon the Co-Co distance (Table 5, Fig. 2) has a non-pattered character, whereas the energy dependence of the  $\eta^2:\eta^2:\eta^2/\eta^{2'}$  ones has maximum exactly at the middle of Co

pathway (Table 6 and Fig. 2). The energies of the  $\eta^2:\eta^2:\eta^2/\eta^2$  structures are 8 – 13 kcal/mol lower than the  $\eta^2:\eta^2:\eta^2/\eta^{2'}$  ones.

The linear and bent  $Co_2(C_{60})_3$  structures can be transformed to the  $Co_2(C_{60})_2$  clusters through hopping of cobalt ions among the  $\eta^2$  and  $\eta^{2'}$  sites with, ultimately, the formation of cobalt dimers and subsequent removal of  $C_{60}$  fullerene. The possible reaction pathway of the cobalt ion migrating around the central  $C_{60}$  cage through  $\eta^2/\eta^2:\eta^2/\eta^2$  and  $\eta^2/\eta^2:\eta^2/\eta^{2'}$  sites is presented on Fig. 2 by the color dots and red broken arrows. The colors of the dots reflect relative energies of the isomers and intermediates. The initial positions of both cobalt ions on the opposite sites of the central  $C_{60}$  cage are marked by a  $Co^1$  and a  $Co^2$  symbols (the first and second ions respectively).

Without taking into account the relative orientation of the  $C_{60}$  cages in the  $Co_2(C_{60})_2$  clusters, there are only 3 possible types of cobalt dimer coordinations around the  $C_6$  fragments of the  $C_{60}$  cage. The first one is the global minimum Isomer 1 of  $\eta^2:\eta^2$  type (Table 4, the only one structure). This structure is schematically presented on the Fig. 2 by a broken red line connecting the  $Co^1$  position (red dot) and the brown dot reflecting the final position of the second cobalt ion ( $Co^2$ ).

The second coordination of  $\eta^2:\eta^2$  type (the most representative example is Isomer 2 (relative energy 9.4 kcal/mol) in Table 4) is presented by two red circles connected by a broken red line. This structure can be obtained through the same intermediate state (the dark blue circle) as the Isomer 1. Finally, the last high energy isomer of  $\eta^2:\eta^{2'}$  type (the light blue circle connected to the red  $Co^1$  position by solid red line) can be obtained through alternative reaction pathways starting from the empty blue circles (in reality these positions were not calculated, but the relative energies of the  $\eta^{2'}$  intermediates should be close to the neighboring highest intermediate structure, violet circle, 49.2 kcal/mol).

The formation mechanism of the highest energy  $\eta^2:\eta^2$  structure is really special and proceeds without formation of an intermediate structure neighboring the  $C_6$  fragment (like in the case of two previous clusters). The absence of the corresponding intermediate structure is represented on Fig. 2 by a “Do not stop” traffic sign. The resulting  $Co_2(C_{60})_3$  cluster, number 5 from Table 6 (the analog of Isomer 7 from Table 4), can be characterized by the existence of direct Co-Co chemical bond with a length of 2.530 Å.

The migration of the second cobalt ion ( $Co^2$ ) approaching the first one ( $Co^1$ ) proceeds through a set of isomers and intermediates (see Fig. 2). The energy difference between the initial  $Co_2(C_{60})_3$   $Co^2$  position (pink circle, 35.3 kcal/mol) and the highest energy intermediate (violet circle, 49.2 kcal/mol), located exactly in the middle of the reaction pathway, is equal to 13.9 kcal/mol. From this point, an approaching of the second cobalt ion to the first one leads to the consequent decrease of the energy of the system. After formation of the cobalt dimer, one  $C_{60}$  can be removed from the  $Co_2(C_{60})_3$  system with formation of some kind of  $Co_2(C_{60})_2$  isomer. The formation of the two lowest energy  $Co_2(C_{60})_2$  isomers of  $\eta^2:\eta^2$  and  $\eta^2:\eta^2$  types of coordination (0 kcal/mol and 9.4 kcal/mol) can proceed through the same intermediate state (43.5 kcal/mol, dark blue circle). The absence of  $Co_2(C_{60})_3$  clusters in the mass-spectra of the Co/ $C_{60}$  composites<sup>5</sup> confirms the instability of the species.

*b)  $Co_xC_{60}$  ( $x=3-8$ ) clusters with one  $C_{60}$  site*

Coordination of one  $C_{60}$  cage by a  $Co_x$  core dramatically changes the structure and spin states of TM cores (Table 7). Most  $Co_x$  fragments demonstrate  $\eta^2$  or  $\eta^2'$  types of coordination, but an  $\eta^1$  one can be found as well for the  $Co_8C_{60}$  cluster. The coordination of the  $C_{60}$  cage by a  $Co_x$  part is followed by complete reconstruction of

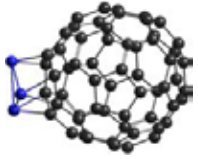
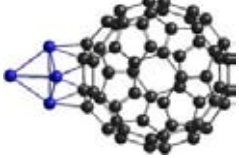
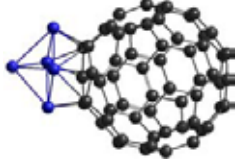
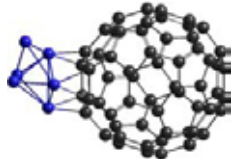
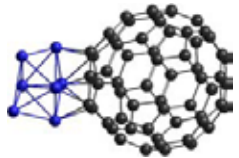
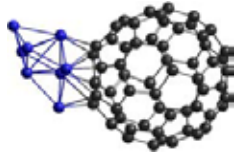
the interface with even a formation of irregular rhombic cobalt facets at the  $Co_xC_{60}$  interface ( $Co_5$ ,  $Co_7$  and  $Co_8$  cores), or transformation of the distorted rhombic  $Co_4$  free-standing cluster to a tetrahedral structure. The atomic coordinates of all  $Co_xC_{60}$  clusters can be downloaded from Supporting Information section of JPCC website.

The Co-C interatomic distances (Table 7) of the  $Co_xC_{60}$  clusters demonstrate strong interactions of the metallic cores with the  $C_{60}$  cage. The experimental Co-C distance in  $Co_x/C_{60}$  species [15] at the lower limit of cobalt concentration is 2.01 Å, whereas the theoretical GGA B3LYP/6-31G\* distance is 2.06 Å [23]. The theoretical GGA PBE/6-31G\* Co-C distances in  $Co_xC_{60}$  clusters demonstrate wide variations of the lengths: from 1.815 to 2.230 Å for the  $Co_8C_{60}$  cluster. The Co-C distances for other  $Co_xC_{60}$  clusters are inside this interval (Table 7). It does directly indicate the wide variation of chemical bonds between the  $Co_x$  cores and the  $C_{60}$  cages with variations of the Co-Co interatomic distances as well.

The electronic correlation effects in rich Co-*d* shells play an important role in determination of the atomic structure features of the  $Co_xC_{60}$  species. Even in the simplest  $Co_3C_{60}$  case (the  $Co_3$  fragment coordinates to the carbon hexagon of the  $C_{60}$  site through three  $\eta^2$  positions) the Jahn-Teller effect leads to complete cancellation of the high initial symmetry of the constituting parts (icosahedral of the  $C_{60}$  cage and  $C_{2v}$  (Table 1) of the  $Co_3$  core) and formation of the  $C_1$  symmetry structure of the  $Co_3C_{60}$  cluster with three nonequivalent Co-C distances (2.439, 2.455 and 2.482 Å, Table 7). It is necessary to note that in the absence of electronic correlations the resulting structure should display  $C_{3v}$  symmetry. Actually, the symmetry of the  $Co_3C_{60}$  cluster is just a strongly distorted  $C_{3v}$  group. The GGA PBE/6-31G\* results correlate well with the Co-Co distances



Table 7. Type of coordination, Co-C and Co-Co interatomic distances (Å) and the number of unpaired spins of the ground states of the  $\text{Co}_x\text{C}_{60}$  clusters

$\text{Co}_x$ core	General view	Type of coordination	Interatomic Co-C distances, Å	Interatomic Co-Co distances, Å	Number of unpaired spins (spin/atom)
$\text{Co}_3$		$\eta^2/\eta^2/\eta^2$	1.951-1.848	2.482-2.439	7 (2.33)
$\text{Co}_4$		$\eta^2/\eta^2/\eta^2$	1.920-1.882	2.695-2.364	10 (2.5)
$\text{Co}_5$		$\eta^2/\eta^2/\eta^2/\eta^2$	2.093-1.833	2.704-2.268	11 (2.2)
$\text{Co}_6$		$\eta^2/\eta^2/\eta^2$	1.903-1.870	2.621-2.291	12 (2)
$\text{Co}_7$		$\eta^2/\eta^2/\eta^2/\eta^2$	2.161-1.818	2.889-2.96	15 (2.14)
$\text{Co}_8$		$\eta^2/\eta^2/\eta^1/\eta^2$	2.230-1.815	2.810-2.171	12 (1.5)

in  $\text{Co}_2(\text{C}_{60})_2$  isomers at the GGA B3LYP/6-31G\* level of theory (2.41-2.98 Å) [54].

The  $\text{Co}_4\text{C}_{60}$  cluster with tetrahedral coordination of the cobalt core displays relatively less geometric distortions with resulting  $C_s$  symmetry (Table 7). As in the case of the  $\text{Co}_3\text{C}_{60}$  cluster, the  $\text{Co}_3$  fragment of  $\text{Co}_4$  core is coordinated to the carbon hexagon through three  $\eta^2$  sites. These correlations

distort the ideal  $C_{3v}$  group to a  $C_s$  symmetry structure with three nonequivalent Co-C distances (1.920, 1.900 and 1.883 Å). One more  $\text{Co}_x\text{C}_{60}$  cluster with an even number of cobalt ions and tetrahedral cobalt coordination ( $\text{Co}_6\text{C}_{60}$ ) also displays  $C_s$  symmetry (Table 7). As in the cases of  $\text{Co}_3$  and  $\text{Co}_4$  cores, the  $\text{Co}_6$  fragments coordinates to the carbon hexagon of the  $\text{C}_{60}$  ligand through three  $\eta^2$  sites with

three nonequivalent Co-C distances (1.871, 1.892 and 1.903 Å).

All other  $\text{Co}_x$  clusters ( $\text{Co}_5$ ,  $\text{Co}_7$  and  $\text{Co}_8$ ) form distorted rhombic interfaces (Table 7) with complex types of coordinations of TM core fragments with the  $\text{C}_{60}$  site:  $\eta^2/\eta^2/\eta^2/\eta^{2'}$  ( $\text{Co}_5$  and  $\text{Co}_7$ ) and  $\eta^2/\eta^2/\eta^1/\eta^{2'}$  ( $\text{Co}_8$ ). The Jahn-Teller effect completely destroys the symmetry of the clusters with formation of strongly distorted  $\text{C}_1$  structures with wide variations of the Co-C distances (Table 7).

The number of unpaired spins per cobalt ion displays a non-monotonic dependence with two maxima ( $\text{Co}_4$  and  $\text{Co}_7$  cores, Fig. 1). For all  $\text{Co}_x\text{C}_{60}$  clusters spin density is mainly localized at  $\text{Co}_x$  fragments. Different behavior of the spin states in comparison with free-standing  $\text{Co}_n$  clusters (Table 1, Fig. 1) clearly demonstrates the main role of complex bond formation in determination of the non-monotonic behavior of average number of unpaired spins per cobalt atom in the complexes. The  $\text{C}_{60}$  cage significantly changes the chemical state of the cobalt ions with total reconstruction of the atomic and electronic structures of the  $\text{Co}_x$  cores due to oxidation of all or some cobalt atoms. Only for the  $\text{Co}_4\text{C}_{60}$  and  $\text{Co}_7\text{C}_{60}$  species the average number of unpaired spins per cobalt atom is equal to the corresponding  $\text{Co}_4$  and  $\text{Co}_7$  clusters. In other cases the formation of the complex Co-C bonds leads to noticeable decrease in the average number of unpaired spins.

### c) $\text{Co}_x(\text{C}_{60})_2$ ( $x=3-8$ ) nanoclusters

The structural data and spin states for  $\text{Co}_x(\text{C}_{60})_2$  clusters are summarized in Table 8. Coordination of the second  $\text{C}_{60}$  cage by the TM cores consequently changes the structure and spin states of cobalt nanoparticles. As in the case of the  $\text{Co}_x\text{C}_{60}$  clusters, the TM cores demonstrate  $\eta^1$ ,  $\eta^2$  and  $\eta^{2'}$  types of coordination. The coordination of the second  $\text{C}_{60}$  cage by the TM part is followed by similar reconstruction of the interface region

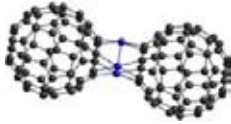
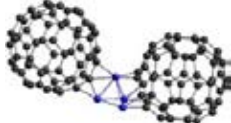
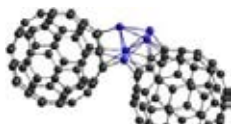
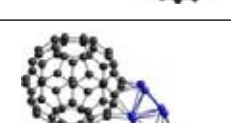
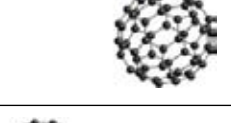
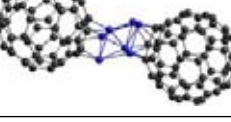
with formation of the additional tetragonal ( $\text{Co}_3$ ,  $\text{Co}_4$ ,  $\text{Co}_5$ ,  $\text{Co}_6$  and  $\text{Co}_7$  cores) or irregular rhombic ( $\text{Co}_7$ ) cobalt facets. It is necessary to note, that for the  $\text{Co}_5(\text{C}_{60})_2$  cluster a state with 9 unpaired spins is only 0.2 kcal/mol higher in energy than the lowest energy isomer with multiplicity equal to 8 (7 unpaired spins). The atomic coordinates of all nanoclusters can be downloaded from Supporting Information section of JPCC website.

The Co-C interatomic distances (Table 8) of the  $\text{Co}_x(\text{C}_{60})_2$  species demonstrate strong interactions between the metallic cores and the  $\text{C}_{60}$  cage with wide variations the distances from 1.846 to 2.125 Å for the  $\text{Co}_5(\text{C}_{60})_2$  cluster. The Co-Co distances are also influenced by formation of complex bonds with the second  $\text{C}_{60}$  cage, with a noticeable decrease in the difference between the maximal (2.696 Å) and minimal (2.201 Å) values compared with the  $\text{Co}_x\text{C}_{60}$  species (2.889 and 2.171 Å, respectively, Table 7).

The electronic correlation effects in rich Co-*d* shells plays the leading role in determination of the main features of the atomic structure of the  $\text{Co}_x(\text{C}_{60})_2$  species. Only the  $\text{Co}_3(\text{C}_{60})_2$  cluster displays low  $\text{C}_2$  symmetry (the  $\text{Co}_3$  fragment coordinates to the carbon hexagons of the  $\text{C}_{60}$  sites through three  $\eta^2$  positions). The  $\text{C}_1$  symmetry group of  $\text{Co}_8(\text{C}_{60})_2$  cluster is in fact a strongly distorted  $\text{C}_2$  group. All other clusters have no symmetry due to Jahn-Teller distortions of their atomic structure. The GGA PBE/6-31G\* results for  $\text{Co}_x(\text{C}_{60})_2$  species also correlate well with the Co-Co distances in  $\text{Co}_2(\text{C}_{60})_2$  isomers at the GGA B3LYP/6-31G\* level of theory (2.98-2.41 Å) [54].

The formation of the complex bonds with the second  $\text{C}_{60}$  site undergoes through the same coordination types (Table 8) between the TM cores and  $\text{C}_{60}$  cages. As in the case of  $\text{Co}_x\text{C}_{60}$ , the most favorable is  $\eta^2/\eta^2/\eta^2$  coordination of a cobalt triangle by a  $\text{C}_6$  fragment of  $\text{C}_{60}$  cage. Also,  $\eta^{2'}$  and  $\eta^1$  types of coordination in different combinations can be found (Table

Table 8. Type of coordination, Co-C and Co-Co interatomic distances (Å) and the number of unpaired spins of the ground states of the  $\text{Co}_x(\text{C}_{60})_2$  clusters

$\text{Co}_x$ core	General view	Type of coordination	Interatomic Co-C distances, Å	Interatomic Co-Co distances, Å	Number of unpaired spins (spin/atom)
$\text{Co}_3$		$\eta^2/\eta^2/\eta^2$ $\eta^2/\eta^2/\eta^2$	1.976-1.965	2.646-2.629	3 (1)
$\text{Co}_4$		$\eta^2/\eta^2/\eta^2$ $\eta^2/\eta^2$	2.120-1.881	2.629-2.345	8 (2)
$\text{Co}_5$		$\eta^2/\eta^2/\eta^2/\eta^2$ $\eta^2/\eta^2/\eta^2$	2.125-1.846	2.860-2.201	7 (1.4)
$\text{Co}_6$		$\eta^2/\eta^2/\eta^2/\eta^2$ $\eta^2/\eta^2/\eta^1/\eta^2$	2.094-1.885	2.549-2.321	12 (2)
$\text{Co}_7$		$\eta^2/\eta^2/\eta^2$ $\eta^2/\eta^1/\eta^1/\eta^1$	1.944-1.865	2.653-2.208	13 (1.86)
$\text{Co}_8$		$\eta^2/\eta^2/\eta^1/\eta^2$ $\eta^2/\eta^1/\eta^2/\eta^1$	2.096-1.845	2.696-2.239	18 (2.25)

8). The most complex case is coordination of the cobalt core of the  $\text{Co}_8(\text{C}_{60})_2$  cluster to the  $\text{C}_{60}$  sites. The interface regions are in fact non-equivalent strongly distorted rhombuses with unique geometry and different types of coordination ( $\eta^2/\eta^2/\eta^1/\eta^2$  and  $\eta^2/\eta^1/\eta^2/\eta^1$ ). The unique atomic structure of the  $\text{Co}_8(\text{C}_{60})_2$  cluster is the direct consequence of the Jahn-Teller distortions caused by electronic correlations in rich Co  $d$ -shells.

For all  $\text{Co}_x(\text{C}_{60})_2$  clusters the main part of spin density is also localized at  $\text{Co}_x$  fragments. The number of unpaired spins per cobalt ion displays non-monotonic dependence with three maxima ( $\text{Co}_4$ ,  $\text{Co}_6$  and  $\text{Co}_8$  cores, Fig. 1). Different behavior of the spin states of free-standing  $\text{Co}_x$ ,  $\text{Co}_x\text{C}_{60}$  and  $\text{Co}_x(\text{C}_{60})_2$  clusters (Tables 1, 7, 8, Fig. 1) clearly demonstrates the main role of complex bond formation in determination of the magnetic properties of the  $\text{Co}_x/\text{C}_{60}$  composites. Formation

of complex bonds between the second  $C_{60}$  cage with  $Co_x$  clusters is favorable to enhance the average number of unpaired spins per cobalt atom due to electron charge transfer from cobalt ions to the  $C_{60}$  cages.

### Conclusions

The atomic structure and relative energetic stability of a wide set of neutral and positively charged  $Co_n(C_{60})_m$  ( $n=1-8$ ,  $m=1-3$ ) clusters with all possible coordinations of cobalt ions and  $C_{60}$  cages in different spin states ( $S=0$ ,  $1/2$ ,  $1$  and  $3/2$ ) were determined based on the GGA/6-31G\* calculations. Theoretical results directly confirm the existing experimental structural data for the  $Co_x/C_{60}$  species. Results indicate that the  $\eta^2$  type of coordination is energetically preferable for all combinations of  $m$  and  $n$  numbers. For the neutral systems with  $n=1$  the low spin state  $S=1/2$  is energetically preferable. For the  $n=2$  cases, the intermediate  $S=1$  spin state is preferable. It was shown that, for the  $n=2$  case, the formation of the cobalt dimers is energetically preferable and can be realized through cobalt ion hopping between the  $\eta^2$  (6-6 edge) and  $\eta^1$  (6-5 edge) sites of  $C_{60}$  cages. The  $\eta^2$  types of structures as well

as the  $\eta^5$  type of structures - and mixed ones - can be realized in the complex  $Co_x/C_{60}$  mixtures during chemical synthesis as intermediate states and high energy isomers.

In most cases the formation of the  $Co_x/C_{60}$  ( $x=3-8$ ) interfaces is followed by complete structural reconstruction of the TM cores. The  $Co_x$  fragments are bonded with a  $C_6$  fragment of the  $C_{60}$  cages through distorted triangular or rhombic interface structures. The individual cobalt ions at the interface regions display  $\eta^2$ ,  $\eta^1$ , or  $\eta^0$  types of coordination. The electron correlations lead to significant structural distortions with complete destroying of initial high-symmetry structures of constituting parts. The formation of complex bonds with one  $C_{60}$  cage leads to non-monotonic dependence of average number of unpaired spins per cobalt atom. The attaching of the second  $C_{60}$  site to a  $Co_x$  core leads to consequent changes of the electronic structure, increasing the average number of unpaired spins. The obtained theoretical data can be used to synthesize novel  $nc-Co/Co_x(C_{60})_y$  compounds with optimized magnetic properties varying the  $Co/C_{60}$  content and synthesis conditions.

### References

1. Bader, S.D., Advances in Nanomagnetism via X-ray Techniques (REVIEW), Rev. Mod. Phys. 2006, 78, 1-15.
2. Bansmann, J.; Baker, S.H.; Binns, C.; Blackman, J.A.; Bucher, J.-P.; Dorantes-Dávila, J.; Dupuis, V.; Favre, L.; Kechrakos, D.; Kleibert, A.; Meiwes-Broer K.-H.; Pastor, G.M.; Perez, A.; Toulemonde, O.; Trohidou, K.N.; Tuaille, J.; Xie, Y., Magnetic and structural properties of isolated and assembled clusters, Surf. Sci. Rep. 2005, 56, 189-275.
3. Stearns, M. B. On the Origin of Ferromagnetism and the Hyperfine Fields in Fe, Co, and Ni Phys. Rev. B 1973, 8, 4383-4398.
4. Sakai, S.; Yakushiji, K.; Mitani, S.; Takanashi, K.; Naramoto, H.; Avramov, P.V.; Narumi, K.; Lavrentiev, V.I., Tunnel magnetoresistance in Co nanoparticle/Co-C60 compound hybrid system, Appl. Phys. Lett. 2006, 89, 113118-113124.
5. Sakai S.; Sugai I.; Mitani S.; Takanashi K.; Matsumoto Y.; Naramoto H.; Avramov P.V.; Okayasu S.; Maeda Y., Giant tunnel magnetoresistance in codeposited fullerene-cobalt films in the low bias-voltage regime, Appl. Phys. Lett. 2007, 91, 242104-242110.
6. Sakai S.; Yakushiji K.; Mitani S.; Sugai I.; Takanashi K.; Naramoto H.; Avramov P.V.; Lavrentiev V.; Narumi K.; Maeda Y., Magnetic and Magnetotransport Properties in

Nanogranular Co/C60-Co Film with High Magnetoresistance, *Materials Transactions*, 2007, 48, 754-758.

7. Lavrentiev V.; Naramoto H.; Narumi K.; Sakai S., Avramov P., Planar doping of crystalline fullerene with cobalt, *Chem. Phys. Lett.* 2006, 423, 366-370.
8. Dumas-Bouchiat, F.; Nagaraja, H.S.; Rossignol, F.; Champeaux; C., Troliard; G., Catherinot, A.; Givord, D. Cobalt cluster-assembled thin films deposited by low energy cluster beam deposition: Structural and magnetic investigations of deposited layers, *J. Appl. Phys.* 2006, 100, 064304-064311.
9. Morel, R.; Brenac, A.; Portemont, C.; Deutsch, T.; Notin, L., Magnetic anisotropy in icosahedral cobalt clusters, *J. Mag. & Mag. Mat.* 2007, 308, 296-304.
10. Xu, X.; Yin, S.; Moro, R; de Heer, W.A. , Magnetic Moments and Adiabatic Magnetization of Free Cobalt Clusters, *Phys. Rev. Lett.* 2005, 95, 237209-237212.
11. Billas, I.M.L.; Châtelain, A.; de Heer, W.A. , Magnetism from the Atom to the Bulk in Iron, Cobalt, and Nickel Clusters, *Science* 1994, 265, 1682-1684.
12. Billas, I.M.L.; Châtelain, A.; de Heer, W.A., Magnetism of Fe, Co and Ni clusters in molecular beams, *J. Mag. & Mag. Mat.* 1997, 168, 64-84.
13. Högberg, H.; Malm, J.-O.; Talyzin, A.; Norin, L.; Lu, J.; Jansson, U., Deposition of Transition Metal Carbides and Superlattices Using C60 as Carbon Source, *J. Electrochem. Soc.* 2000, 147, 3362-3369.
14. Pedio, M.; Hevesti, K.; Zema, N.; Capozzi, M.; Perfetti, P.; Goutebaron, R.; Pireaux, J.-J.; Caudano, R.; Rudolf, P., C60/metal surfaces: adsorption and decomposition, *Surf. Sci.* 1999, 437, 249-260.
15. Sakai, S.; Naramoto, H.; Lavrentiev, V.; Narumi, K.; Maekawa, M.; Kawasuso, A.; Yaita, T.; Baba, Y., Polymeric Co-C60 Compound Phase Evolved in Atomistically Mixed Thin Films, *Materials Transactoins* 2005, 46, 765-768.
16. Kurikawa, T.; Nagao, S.; Miyajima, K.; Nakajima, A.; Kaya, K., Formation of Cobalt–C60 Clusters: Tricapped Co(C60)3 Unit, *J. Phys. Chem. A* 1998, 102, 1743.
17. Sokolov, V. I., Buckminsterfullerene as a ligand of variable hapticity. Symmetry analysis of possible combinations of face pairs and its consequence for chiral stereochemistry of C60, *Pure & Appl. Chem.* 1998, 70, 789-792.
18. Neretin, I.S.; Slovokhotov, Yu. I., Chemical crystallography of fullerenes, *Russian Chemical Reviews* 2004, 73, 455-571.
19. Arce, M.J.; Viado, A.L.; An, Y.-Z.; Khan, S.I.; Rubin, Y., Triple Scission of a Six-Membered Ring on the Surface of C60 via Consecutive Pericyclic Reactions and Oxidative Cobalt Insertion, *J. Am. Chem. Soc.* 1996, 118, 3775-3776.
20. Jiao, Q.; Huang, Y.; Lee, S.; Gord, J.R.; Freiser, B.S., The unique gas-phase reactivity of C60+ and C70+ with iron-pentacarbonyl, *J. Am. Chem. Soc.* 1992, 114, 2726-2727.
21. Sawamura, M.; Iikura, H.; Nakamura, E., The First Pentahaptofullerene Metal Complexes, *J. Am. Chem. Soc.* 1996, 118, 12850-12851.
22. Nakamura, E.; Sawamura, M., Chemistry of  $\eta^5$ -fullerene metal complexes, *Pure & Appl. Chem.* 2001, 73, 355-359.
23. Nagao, S.; Kurikawa, T.; Miyajima, K.; Nakajima, A.; Kaya, K., Formation and Structures of Transition Metal–C60 Clusters, *J. Am. Chem. Soc.* 1998, 102, 4495-4500.
24. Sokolov, V.I. Buckminsterfullerene as a ligand of variable hapticity. Symmetry analysis of possible combinations of face pairs and its consequence for chiral stereochemistry of C60, *Dokl. Akad. Nauk*, 1992, 326, 647-649.

25. Rashinkangas, M.; Pakkanen, T.T., Multimetallic binding to fullerenes: C<sub>60</sub>{Ir<sub>2</sub>Cl<sub>2</sub>(1,5-COD)<sub>2</sub>}<sub>2</sub>. A novel coordination mode to fullerenes, *J. Am. Chem. Soc.* 1993, 115, 4901-4912.
26. Guldi, D.M.; Maggini, M.; Menna, E.; Scorrano, G.; Ceroni, P.; Marcaccio, M.; Paolucci, F.; Roffia, S., A Photosensitizer Dinuclear Ruthenium Complex: Intramolecular Energy Transfer to a Covalently Linked Fullerene Acceptor, *Chem. Eur. J.* 2001, 7(8), 1597-1605.
27. Hsu, H.-F.; Shapley, J. R., Ru<sub>3</sub>(CO)<sub>9</sub>(m<sup>3</sup>-h<sub>2</sub>,h<sub>2</sub>,h<sub>2</sub>-C<sub>60</sub>): A Cluster Face-Capping, Arene-Like Complex of C<sub>60</sub>, *J. Am. Chem. Soc.* 1996, 118, 9192-9193.
28. Lee, K.; Song, H.; Kim, B.; Park, J.T.; Park, S.; Choi, M.-G., The First Fullerene–Metal Sandwich Complex: An Unusually Strong Electronic Communication between Two C<sub>60</sub> Cages, *J. Am. Chem. Soc.* 2002, 124, 2872-2873.
29. Andriotis, A.N.; Menon, M., Geometry and bonding in small (C<sub>60</sub>)<sub>n</sub>Nim clusters' *Phys. Rev.* 1999, B60, 4521-4529.
30. Andriotis, A.N.; Menon, M.; Froudakis, G.E., Contrasting bonding behaviors of 3-d transition metal atoms with graphite and C<sub>60</sub>, *Phys. Rev.* 2000, B62, 9867-9875.
31. Xu, Z.-F.; Xie, Y.; Feng, W.-L.; Shaefer III, H.F., Systematic Investigation of Electronic and Molecular Structures for the First Transition Metal Series Metallocenes M(C<sub>5</sub>H<sub>5</sub>)<sub>2</sub> (M = V, Cr, Mn, Fe, Co, and Ni), *J. Phys. Chem. A* 2003, 107, 2716-2729.
32. Pederson, M.R.; Jackson, K.A.; Boyer, L.L., Enhanced stabilization of Ceo crystals through doping, *Phys. Rev.* 1992, B45, 6919-6922.
33. Dolg, M., Combined Pseudopotential and Density Functional Study of Bis-η<sup>6</sup>-benzene d and f Element Complexes, *J. Chem. Inf. Comput. Sci.* 2001, 41, 18-21.
34. Rösch, N.; Hoffmann, R., Geometry of transition metal complexes with ethylene or allyl groups as the only ligands, *Inorg. Chem.* 1974, 13, 2656-2666.
35. Tian, Z.; Tang, Z., Experimental and theoretical studies of the interaction of silver cluster cations Ag<sub>n</sub><sup>+</sup> (n = 1-4) with ethylene, *Rapid Commun. Mass Spectrom.* 2005, 19, 2893-2904.
36. Stankevich, I.V.; Chistyakov, A.L., Metal complexes of allyl derivatives of C<sub>60</sub> fullerene: molecular and electronic structure prediction from density functional calculations, *Russ. Chem. Bull., Int. Edition* 2003, 52, 1, 1272-1279
37. Stankevich, I.V.; Chistyakov, A.L., On Some Complexes of Allyl Derivatives of C<sub>60</sub> Fullerene: Simulation of Molecular and Electron Structure by DFT, *Fullerenes, Nanotubes and Carbon Nanostructures* 2004, 12, 431-435.
38. Ramaniah, L.M.; Boero, M.; Laghate, M., Tantalum-Fullerene Clusters: A First-Principles Study of Static Properties and Dynamical Behavior, *Phys. Rev.* 2004, B70, 035411-1.
39. Gaussian 03, Revision C.02, Frisch, M. J.; Trucks, G. W.; Schlegel, H. B.; Scuseria, G. E.; Robb, M. A.; Cheeseman, J. R.; Montgomery, Jr., J. A.; Vreven, T.; Kudin, K. N.; Burant, J. C.; Millam, J. M.; Iyengar, S. S.; Tomasi, J.; Barone, V.; Mennucci, B.; Cossi, M.; Scalmani, G.; Rega, N.; Petersson, G. A.; Nakatsuji, H.; Hada, M.; Ehara, M.; Toyota, K.; Fukuda, R.; Hasegawa, J.; Ishida, M.; Nakajima, T.; Honda, Y.; Kitao, O.; Nakai, H.; Klene, M.; Li, X.; Knox, J. E.; Hratchian, H. P.; Cross, J. B.; Bakken, V.; Adamo, C.; Jaramillo, J.; Gomperts, R.; Stratmann, R. E.; Yazyev, O.; Austin, A. J.; Cammi, R.; Pomelli, C.; Ochterski, J. W.; Ayala, P. Y.; Morokuma, K.; Voth, G. A.; Salvador, P.; Dannenberg, J. J.; Zakrzewski, V. G.; Dapprich, S.; Daniels, A. D.; Strain, M. C.; Farkas, O.; Malick, D. K.; Rabuck, A. D.; Raghavachari, K.;

- Foresman, J. B.; Ortiz, J. V.; Cui, Q.; Baboul, A. G.; Clifford, S.; Cioslowski, J.; Stefanov, B. B.; Liu, G.; Liashenko, A.; Piskorz, P.; Komaromi, I.; Martin, R. L.; Fox, D. J.; Keith, T.; Al-Laham, M. A.; Peng, C. Y.; Nanayakkara, A.; Challacombe, M.; Gill, P. M. W.; Johnson, B.; Chen, W.; Wong, M. W.; Gonzalez, C.; and Pople, J. A. Gaussian, Inc., Wallingford CT, 2004.
40. a) Becke A.D., Density-functional exchange-energy approximation with correct asymptotic behaviour, *Phys. Rev. A* 38 1988 pp3098-3100 b) C. Lee, W. Yang, and R.G. Parr Development of the Colle-Salvetti correlation-energy formula into a functional of the electron density, *Phys. Rev. B* 37 (1988) 785-789 c) Barone, V., Inclusion of Hartree-Fock exchange in the density functional approach. Benchmark computations for diatomic molecules containing H, B, C, N, O, and F atoms, *Chem. Phys. Lett.*, 1994, 226, 392-398.
  41. Perdew, J.P.; Burke, K.; Ernzerhof, M., Generalized Gradient Approximation Made Simple, *Phys. Rev. Lett.* 1996, 77 3865-3868.
  42. Perdew, J.P.; Burke, K.; Ernzerhof, M., Generalized Gradient Approximation Made Simple [*Phys. Rev. Lett.* 77, 3865 (1996)] *Phys. Rev. Lett.* 1997, 78, 1396-1396.
  43. Avramov, P. V.; Scuseria G. E.; Kudin, K., Single wall carbon nanotubes density of states: comparison of experiment and theory, *Chem. Phys. Lett.* 2003, 370, 597-601.
  44. Petersson, G.A.; Malick, D.K.; Wilson, W.G.; Ochterski, J.W.; Montgomery, J.A.; Frisch, M.J., Calibration and comparison of the Gaussian-2, complete basis set, and density functional methods for computational thermochemistry, *J. Chem. Phys.* 1998, 109, 10570-10574.
  45. Wang, X.J.; Wong, L.H.; Hu, L.H.; Chan, C.Y.; Su, Z.; Chen, G.H., Improving the Accuracy of Density-Functional Theory Calculation: The Statistical Correction Approach, *J. Phys. Chem. A* 2004, 108, 8514-8525.
  46. Ernzerhof, M.; Scuseria, G.E., Assessment of the Perdew–Burke–Ernzerhof exchange-correlation functional, *J. Chem. Phys.* 1999, 110, 5029-5034.
  47. Adamo, C.; Barone, V., Toward reliable density functional methods without adjustable parameters: The PBE0 model, *J. Chem. Phys.* 1999, 110, 6158-6167.
  48. Rodríguez-López, J.L.; Aguilera-Granja, F.; Michaelian, K.; Vega, A., Magnetic structure of cobalt clusters, *J. Al. & Comp.* 2004, 396, 93-96.
  49. Ma, Q.-M.; Xie, Z.; Wang, J.; Liu, Y.; Li, Y.-C., Structures, stabilities and magnetic properties of small Co clusters, *Phys. Lett. A* 2006, 358, 289-296.
  50. Ma, Q.-M.; Liu, Y.; Xie, Z.; Wang, J., Ab initio Study of Geometries and Magnetic Properties of Small Co Clusters, *J. Phys.: Conf. Series* 2006, 29, 163-166.
  51. Rodríguez-López, J.L.; Aguilera-Granja, F.; Michaelian, K.; Vega, A., Structure and magnetism of cobalt clusters, *Phys. Rev. B* 2003, 67, 174413-174419.
  52. Eletsii, A. V.; Smirnov, B., Fullerenes and Carbon Structures, *M. Physics-USpekhi* 1995, 38, 935-978.
  53. Andreoni, W., Computational approach to the physical chemistry of fullerenes and their derivatives, *Annu. Rev. Phys. Chem.* 1998, 49, 405-439.
  54. Avramov P.V.; Naramoto H.; Sakai S.; Narumi K.; Lavrentiev V.; Maeda Y., Quantum Chemical Study of Atomic Structure Evolution of Cox/C60 ( $x \leq 2.8$ ) Composites, *J. Phys. Chem. A* 2007, 111, 2299-2306.